



Longitudinal assessment of placental perfusion in normal and hypertensive pregnancies using pseudo-continuous arterial spin-labeled MRI: preliminary experience

Christina L. Herrera^{1,2} · Yiming Wang³ · Durga Udayakumar^{3,4} · Yin Xi^{3,5} · Quyen N. Do³ · Matthew A. Lewis³ · David M. Owen^{1,2} · Baowei Fei^{3,4,6} · Catherine Y. Spong^{1,2} · Diane M. Twickler^{1,2,3} · Ananth J. Madhuranthakam^{3,4}

Received: 7 August 2022 / Revised: 5 May 2023 / Accepted: 17 May 2023 / Published online: 19 July 2023
© The Author(s), under exclusive licence to European Society of Radiology 2023

Abstract

Objectives To evaluate longitudinal placental perfusion using pseudo-continuous arterial spin-labeled (pCASL) MRI in normal pregnancies and in pregnancies affected by chronic hypertension (cHTN), who are at the greatest risk for placental-mediated disease conditions.

Methods Eighteen normal and 23 pregnant subjects with cHTN requiring antihypertensive therapy were scanned at 3 T using free-breathing pCASL-MRI at 16–20 and 24–28 weeks of gestational age.

Results Mean placental perfusion was 103.1 ± 48.0 and 71.4 ± 18.3 mL/100 g/min at 16–20 and 24–28 weeks respectively in normal pregnancies and 79.4 ± 27.4 and 74.9 ± 26.6 mL/100 g/min in cHTN pregnancies. There was a significant decrease in perfusion between the first and second scans in normal pregnancies ($p = 0.004$), which was not observed in cHTN pregnancies ($p = 0.36$). The mean perfusion was not statistically different between normal and cHTN pregnancies at both scans, but the absolute change in perfusion per week was statistically different between these groups ($p = 0.044$). Furthermore, placental perfusion was significantly lower at both time points ($p = 0.027$ and 0.044 respectively) in the four pregnant subjects with cHTN who went on to have infants that were small for gestational age (52.7 ± 20.4 and 50.4 ± 20.9 mL/100 g/min) versus those who did not (85 ± 25.6 and 80.0 ± 25.1 mL/100 g/min).

Conclusion pCASL-MRI enables longitudinal assessment of placental perfusion in pregnant subjects. Placental perfusion in the second trimester declined in normal pregnancies whereas it remained unchanged in cHTN pregnancies, consistent with alterations due to vascular disease pathology. Perfusion was significantly lower in those with small for gestational age infants, indicating that pCASL-MRI-measured perfusion may be an effective imaging biomarker for placental insufficiency.

Clinical relevance statement pCASL-MRI enables longitudinal assessment of placental perfusion without administering exogenous contrast agent and can identify placental insufficiency in pregnant subjects with chronic hypertension that can lead to earlier interventions.

Key Points

- Arterial spin-labeled (ASL) magnetic resonance imaging (MRI) enables longitudinal assessment of placental perfusion without administering exogenous contrast agent.
- ASL-MRI-measured placental perfusion decreased significantly between 16–20 week and 24–28 week gestational age in normal pregnancies, while it remained relatively constant in hypertensive pregnancies, attributed to vascular disease pathology.
- ASL-MRI-measured placental perfusion was significantly lower in subjects with hypertension who had a small for gestational age infant at 16–20-week gestation, indicating perfusion as an effective biomarker of placental insufficiency.

Authors Christina L. Herrera and Yiming Wang made equal contributions to the article.

✉ Ananth J. Madhuranthakam
Ananth.Madhuranthakam@UTSouthwestern.edu

¹ Department of Obstetrics and Gynecology, UT Southwestern Medical Center, Dallas, TX, USA

² Parkland Health and Hospital System, Dallas, TX, USA

³ Department of Radiology, UT Southwestern Medical Center, 5323 Harry Hines Blvd., Dallas, TX 75390-9061, USA

⁴ Advanced Imaging Research Center, UT Southwestern Medical Center, Dallas, TX, USA

⁵ Department of Clinical Science, UT Southwestern Medical Center, Dallas, TX, USA

⁶ Department of Bioengineering, University of Texas at Dallas, Richardson, TX, USA

Keywords Placenta · Perfusion · Hypertension · Preeclampsia · Perfusion-weighted MRI

Abbreviations

ASL	Arterial spin labeling
BGS	Background suppression
cHTN	Chronic hypertension
FGR	Fetal growth restriction
NSA	Number of signal averages
PBF	Placental blood flow
pCASL	Pseudo-continuous arterial spin-labeled
SGA	Small for gestational age
SPE	Preeclampsia with severe features
SShTSE	Single-shot turbo spin echo

Introduction

The role of the placenta in the pathology of pregnancy-related disease remains incompletely understood [1]. Reduced maternal blood flow to the placenta is thought to contribute to placental complications and animal models have validated this concept with mechanical restriction of blood flow [2, 3]. Doppler ultrasound of pregnant subjects has suggested a role for hypoperfusion in conditions such as preeclampsia and fetal growth restriction (FGR); however, indirect measurements of impedance of the uterine artery correlate poorly with outcome and are of limited predictive value [4, 5].

In recent years, *in vivo* assessment of the placenta has enabled the direct measurement of perfusion using noninvasive techniques such as arterial spin-labeled (ASL) magnetic resonance imaging (MRI). ASL-MRI is appealing as it uses endogenous water in the blood as a tracer for perfusion and has led to several recent applications in human pregnancy [6–10]. The ability of ASL-MRI to measure placental perfusion in pregnant subjects with chronic hypertension (cHTN) will be valuable, since these patients are at an increased risk for placental-mediated diseases. One in 3 pregnant subjects with cHTN deliver preterm from complications of superimposed preeclampsia or FGR [11]. Compared to normal subjects, the placenta of the hypertensive subjects appears to have increased resistance in the uterine artery, suggesting decreased perfusion. Additionally, morphologic studies of placental histology have indicated that pregnancies complicated with preeclampsia and FGR are characterized by defective remodeling of the spiral arteries [12–14]. Collectively, this argues that perfusion in hypertensive placentas should be

altered compared to normal placentas, and perhaps even more so in the setting of superimposed placental-mediated disease.

Thus, the purpose of our study was to evaluate longitudinal placental perfusion using pseudo-continuous arterial spin-labeled (pCASL) MRI in normal pregnancies and in pregnancies affected by cHTN, who are at the greatest risk for placental-mediated disease conditions of preeclampsia and FGR. We hypothesized that the baseline perfusion in hypertensive placentas was lower than in normal placentas and that this decreased perfusion persisted longitudinally over time. Furthermore, we also hypothesized that even greater reduction of perfusion would be observed in pregnancies with the development of superimposed placental-mediated diseases such as preeclampsia and FGR.

Materials and methods

Study population

This preliminary experience was based on a prospective study approved by the local Institutional Review Board. Study participants were recruited from our hospital system which provides obstetric care to a major metropolitan area. All subjects provided written informed consent before participation and underwent two longitudinal MRI scans at 16–20 and 24–28 weeks of gestational age between March 2019 and September 2022. Inclusion criteria were as follows: pregnant subjects less than 20 weeks' gestational age at recruitment with gestational age confirmed by ultrasonography per standard criteria [15], either healthy or with cHTN requiring antihypertensive therapy,

Table 1 Clinical reference standard definitions

Chronic hypertension (cHTN)	Blood pressure \geq 140/90 mmHg, either before pregnancy or at $<$ 20 weeks gestational age
Preeclampsia with severe features (SPE)	Blood pressure \geq 160/110 mmHg after 20 weeks gestational age plus thrombocytopenia, renal insufficiency, liver involvement, cerebral symptoms, or pulmonary edema
Small for gestational age (SGA)	Birth weight $<$ 10th percentile

singleton gestation, and body mass index $< 40 \text{ kg/m}^2$. Exclusion criteria were as follows: other major maternal medical co-morbidities, known fetal or placental abnormalities, and contraindications or inability to tolerate MRI.

We have used the established definitions for cHTN, preeclampsia with severe features (SPE), and small for gestational age (Table 1) [16–18]. SPE was defined as systolic blood pressure of 160 mm Hg or higher, or diastolic pressure of 110 mm Hg or higher on two occasions at least 4 h apart after 20 weeks of gestation in an individual with a previously normal blood pressure or with new onset of thrombocytopenia, renal insufficiency (serum creatinine greater than 1.1 mg/dL), impaired liver function (elevated liver transaminases to twice the normal concentration), pulmonary edema, or cerebral or visual symptoms [16]. Fetal growth restriction (FGR) was defined as estimated fetal weight less than 10th percentile for expected gestational age. Small for gestational age (SGA) was defined as newborn weight less than 10th percentile for expected newborn weight [18]. The cHTN cohort was restricted to those requiring antihypertensive therapy, as they are at the highest risk for preeclampsia and FGR [19, 20]. Clinical information for maternal and neonatal outcomes was reviewed from the electronic medical record.

MR imaging

Imaging was performed on a 3-T Ingenia MR scanner (Philips Healthcare). Pregnant subjects were placed in the supine, feet-first position [21] with the anterior 16-channel phased array coil, which was used in combination with the

12-channel posterior coil embedded in the table. All subjects were scanned during free breathing. Pseudo-continuous ASL (pCASL) was used for perfusion MRI. We chose pCASL-MRI since it uses a spatially selective labeling approach [22, 23] and reflects the contribution only from the maternal blood supply [8]. Prior to the ASL data acquisition, T2-weighted images were acquired at 5-mm slice thickness in coronal, axial, and sagittal planes to assist in the positioning of the labeling plane and imaging slices. Additional T2-weighted images with the same slice thickness of 10 mm and image coverage as pCASL were also acquired in the oblique-coronal plane to the placenta, prescribed perpendicular to the umbilical cord insertion. The pCASL labeling plane was positioned perpendicularly to the abdominal aorta, right above the level of the aortic bifurcation (Fig. 1).

ASL-MRI sequence

The ASL-MRI sequence consisted of a multi-slice 2D pCASL and a multi-slice proton density-weighted (M_0) acquisition [24, 25]. For pCASL labeling, a train of selective RF pulses (duration = 480 μs , interval = 1210 μs , $B_{1, \text{average}} = 1.07 \mu\text{T}$) and corresponding gradients ($G_{\text{average}} = 0.36 \text{ mT/m}$, $G_{\text{max}} = 5 \text{ mT/m}$) were used. 2D single-shot turbo spin echo (SShTSE) was used for data acquisition. The imaging parameters were as follows: TR/TE = 7500/38 ms, FOV = $275 \times 335 \times 54 \text{ mm}^3$, acquired resolution = $3 \times 3 \text{ mm}^2$, slice thickness = 10 mm, number of signal averages (NSA) = 4, number of slices = 5, echo spacing = 5.5 ms, shot duration = 340 ms, echo train length (ETL) = 62, partial phase-encoding ratio = 0.55 along ky, receiver bandwidth = 307 Hz/pixel, label duration = 1.8 s, post-label delay = 1.8 s, 4 background suppression (BGS) pulses [26],

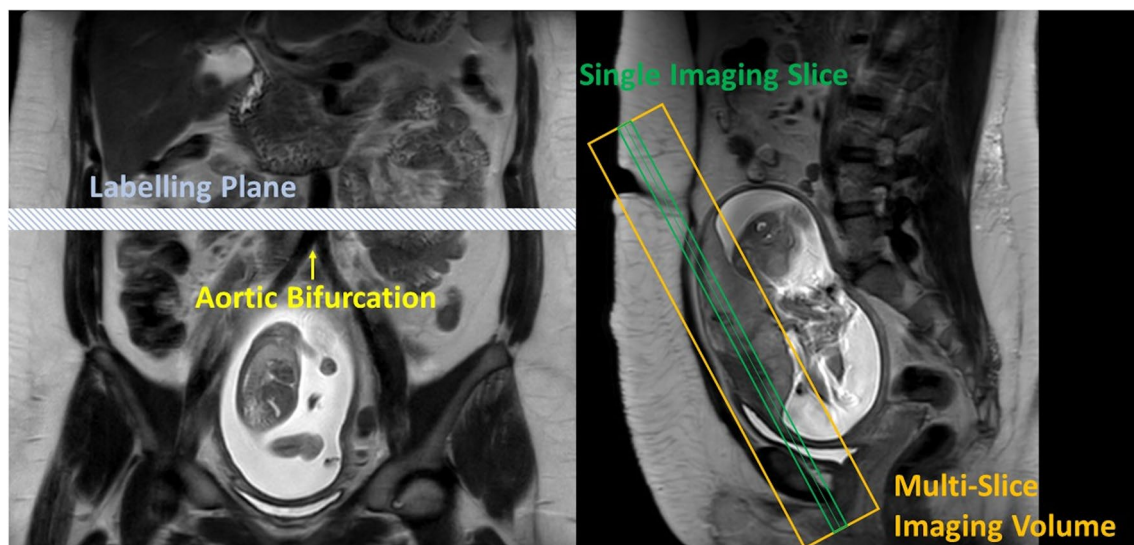


Fig. 1 Coronal (a) and sagittal (b) T2-weighted MR images showing labeling plane and imaging volume of pCASL-MRI for a subject with chronic hypertension at 16-week gestational age (visit 1). The pCASL

labeling plane was placed right above the aortic bifurcation while the image slices covered the entire placenta in an oblique-coronal orientation to the placenta, prescribed perpendicular to the umbilical cord insertion

and total scan time = 5 min. A PLD of 1.8 s was used since it provides an optimal balance between T1 recovery of the labeled blood (~1.6 s T1 at 3 T) and the transit delay from the labeling plane, since the arterial transit time using pCASL-MRI was previously measured to be ~1.3 s [8]. M_0 images were acquired with the same parameters but with single average, without labeling or BGS and in a scan time of 40 s.

Data processing

ASL images were reconstructed using an in-house-developed algorithm implemented on the scanner reconstruction platform (Philips Recon2.0). The custom-built reconstruction performed the complex subtraction between the control and label images in the k-space, followed by Fourier transformation including Homodyne reconstruction to generate the perfusion difference images (ΔM).

The placental blood flow (PBF) values were quantified using the standard model for continuous ASL, given by Eq. 1:

$$\text{PBF} = 6000 \cdot \frac{\Delta M}{M_0} \cdot \frac{\lambda}{2\alpha T_1} \cdot \frac{e^{-\frac{\text{PLD}}{T_1}}}{1 - e^{-\frac{\tau}{T_1}}} \text{ mL/100g/min} \quad (1)$$

where ΔM is the signal intensity of the perfusion difference image; M_0 is the signal intensity of the proton density-weighted image; λ is the blood partition coefficient (0.9); α is the net labeling efficiency (0.6), which is the product of pCASL inversion efficiency (0.9) and an additional inversion efficiency (0.75) by BGS; T_1 is the longitudinal relaxation time of blood at 3 T (1.6 s); PLD is the post-label delay (1.8 s); and τ is the labeling duration (1.8 s). For each subject, PBF quantification was performed using mean M_0 value averaged from a Polygon region of interest (ROI) drawn freehand on the placenta M_0 image.

Data analysis

For each subject, the 5-slice T2-weighted images corresponding to pCASL-MRI acquired at the same location and 10-mm slice thickness were reviewed. From these T2-weighted images, 2 slices that had the most coverage of the placenta were selected. Placenta ROIs were manually drawn on the 2 selected T2-weighted image sequences by YW with 5 years of experience in medical image analysis and reviewed by a radiologist (DMT) with 30 years of MR placental experience. The ROIs were then transferred from the T2-weighted images to the corresponding PBF maps, and the mean PBF value and its standard deviation were calculated from the 2 ROIs.

Statistical analysis

Demographics data were analyzed using unpaired Wilcoxon tests for continuous variables and the Fisher exact

test for categorical variables. All statistical analyses were performed using Prism (GraphPad) and R (R Core Team). Mean and standard deviation (SD) were used to analyze perfusion. Comparisons of perfusion measurement between two gestational ages within each subject were performed using the paired Wilcoxon test, and comparisons between normal and cHTN subjects were performed using the unpaired Mann–Whitney U -test. Absolute changes per week in PBF were defined as $(V_2 - V_1) / (T_2 - T_1)$ where V = visits 1 and 2, and T = gestational age at visits 1 and 2 respectively and compared using the Mann–Whitney U -test. $p < 0.05$ was considered statistically significant.

Results

A total of 52 pregnant subjects, 31 with cHTN and 21 normal, were enrolled and underwent the MRI scans. The second MR exam from 8 pregnant subjects with cHTN and 3 normal pregnant subjects was not available due to the following: failure to keep the appointment (normal = 3), fetal demise (cHTN = 1), unable to undergo a second scan due to the COVID-19 pandemic (cHTN = 2), unable to tolerate exam due to pregnancy-induced nausea (cHTN = 1), and poor imaging quality due to artifacts (cHTN = 4). Longitudinal data were analyzed from the remaining 23 pregnant subjects with cHTN and 18 normal pregnant subjects (Fig. 2).

As anticipated, subjects with cHTN were multiparous and more likely to be obese than their healthier counterparts (all $p < 0.05$) (Table 2). Delivery outcomes were available for only 16 of the normal pregnant subjects since 2 deliveries were performed at outside facilities; however, on a follow-up call, they denied blood pressure issues and reported normal fetal weights for their gestational age at delivery. Hence, the 2 deliveries at outside facilities were considered to be without any pregnancy-related complications for our analysis. Subjects with cHTN were more likely to develop SPE (cHTN: 69.6% [16/23] vs normal: 5.6% [1/18], $p < 0.001$); however, rates of SGA were not significantly different (cHTN: 17.4% [4/23] vs normal: 5.6% [1/18], $p = 0.363$).

A representative example of pCASL-MRI-measured placental perfusion in a normal pregnant subject at 16-week and 28-week gestational age is shown in Fig. 3. Overall, high perfusion is observed at 16 weeks throughout the placenta, which appeared to decrease at 28 weeks along with the enlarging placenta. In contrast, focal hyperintensities representing the spiral arteries are observed with scattered spatial variation in a representative example of placental perfusion in a subject with cHTN (Fig. 4). These focal hyperintensities, representing the perfusion blood flow, appeared scattered at both the 16-week and the 28-week gestational ages.

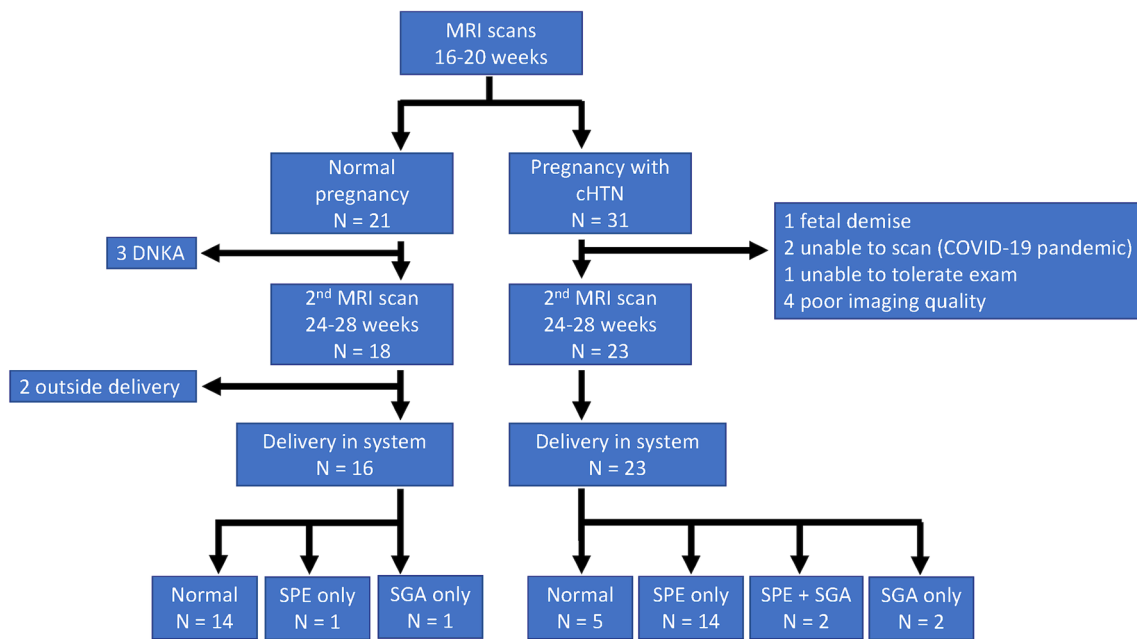


Fig. 2 Flow diagram of the study participants. MRI, magnetic resonance imaging; cHTN, chronic hypertension; DNKA, did not keep appointment; SPE, preeclampsia with severe features; and SGA, small for gestational age

Table 2 Demographics of the study participants included in the perfusion analysis

Baseline characteristics	Normal pregnancy (N=18)	Pregnancy with CHTN (N=23)	p-value
Maternal age (years)	27.6 ± 6.0	30.8 ± 4.8	0.094
≥ 35	4 (22.2%)	7 (30.4%)	0.726
Race/ethnicity			1
Black	4 (22.2%)	5 (21.7%)	
White/Hispanic	14 (77.8%)	18 (78.3%)	
Parity			0.035
0	8 (44.4%)	2 (8.7%)	
1	4 (22.2%)	7 (30.4%)	
≥ 2	6 (33.3%)	14 (60.9%)	
BMI (kg/m ²)			
1st scan	28.9 ± 5.4	34.2 ± 6.3	0.012
2nd scan	30.4 ± 5.0	35.2 ± 6.3	0.016
GA (weeks)			
1st scan	18.0 ± 1.1	18.3 ± 1.4	0.527
2nd scan	26.4 ± 1.3	26.5 ± 1.1	0.693
Obstetrical outcomes			
Delivery GA (weeks)	39.5 ± 1.3	36.1 ± 2.7	<0.001
Birth weight (grams)	3340 [3083, 3810]	2590 [2013, 3198]	0.002
SPE	1 (5.55%)	14 (60.9%)	<0.001
SGA	1 (5.55%)	2 (8.7%)	1
SPE+SGA	0 (0%)	2 (8.7%)	0.5
No complications	16 (88.9%)	5 (21.7%)	<0.001

cHTN, chronic hypertension; GA, gestational age; SPE, preeclampsia with severe features; SGA, small for gestational age. Data reported as N (%), mean ± standard deviation for age, GA, and BMI, and median [1st, 3rd quartile] for birth weight. p-value using unpaired Wilcoxon tests for continuous and the Fisher exact test for categorical variables with p < 0.05 considered statistically significant

Overall, the mean PBF was 103.1 ± 48.0 and 71.4 ± 18.3 mL/100 g/min at 16–20 and 24–28 weeks respectively in the normal pregnant subjects. The corresponding PBF values in pregnant subjects with cHTN were 79.4 ± 27.4 and 74.9 ± 26.6 mL/100 g/min respectively (Fig. 5). There was a statistically significant decrease in perfusion in the normal pregnant subjects between the two time points ($p=0.004$); however, this statistically significant decrease in perfusion was not observed in the pregnant subjects with cHTN ($p=0.360$). The difference in perfusion values between normal pregnant subjects and pregnant subjects with cHTN was not significantly different at 16–20-week ($p=0.139$) or 24–28-week gestational age ($p=0.687$). However, the absolute change in perfusion per week between normal pregnant subjects (-3.37 ± 5.03 mL/100 g/min/week) and pregnant subjects with cHTN (-0.57 ± 2.48 mL/100 g/min/week) was significantly different ($p=0.044$).

In the sub-cohort analysis of pregnant subjects with cHTN (Fig. 6), there was no observed difference in perfusion at either time point among subjects who went on to develop SPE versus those who did not in this limited cohort (all $p > 0.05$). However, there was a statistically significant difference at both time points in the four subjects with cHTN who went on to have infants that were SGA. The mean PBF in the 4 subjects with SGA compared to subjects without SGA were 52.7 ± 20.4 and 85.0 ± 25.6 mL/100 g/min respectively at 16–20-week gestational age ($p=0.027$); and 50.4 ± 20.9 and 80.0 ± 25.1 mL/100 g/min at 24–28-week gestational age ($p=0.044$) (Fig. 6A). Of note, two of these subjects

also had SPE leading to delivery at 31w3d and 36w4d respectively. The third subject was diagnosed with FGR at 28w4d and delivered at 36w0d after the development of concurrent oligohydramnios. The fourth subject delivered at 38w3d in the setting of elevated blood pressure but did not meet the criteria for SPE. The mean PBF was also low in the one normal subject that had an SGA infant at 39w3d and was 57.7 and 46.2 mL/100 g/min at 16–20 and 24–28-week gestational ages respectively. Importantly, the change in perfusion in pregnant subjects with cHTN who had no complications (Fig. 6B, left) was similar to change in perfusion in normal pregnant subjects without cHTN (Fig. 5, left).

Discussion

There are distinct temporal differences in perfusion assessed by pCASL-MRI, as placental development occurs in the normal and chronic hypertension groups. Perfusion in the normal pregnant population decreased over time while the perfusion in the pregnant subjects with cHTN as a combined group remained relatively constant, demonstrating alterations in placental function due to disease pathology. Most interestingly, perfusion was lowest in the subjects with cHTN who went on to have a SGA infant, indicating early second trimester (16–20 weeks of gestational age) placental perfusion may be an effective biomarker for placental insufficiency. Furthermore, the temporal changes in placental perfusion in pregnant subjects with cHTN who had no

Fig. 3 T2-weighted images (left) and ASL perfusion map (right) acquired at the same imaging slice in a normal pregnant subject shown at 16-week (top row) and 28-week (bottom row) gestational ages (GA) respectively. The white dotted line outlines the placenta, drawn on the T2-weighted image and copied over to perfusion map. The arrows represent the vascular signal in the femoral arteries. The residual signal outside the placenta, particularly at 28-week gestational age, shows variations in the background signal. The placental blood flow at visit 1 (top row) was 140 ± 152 mL/100 g/min and at visit 2 (bottom row) was 70 ± 45 mL/100 g/min in this normal subject

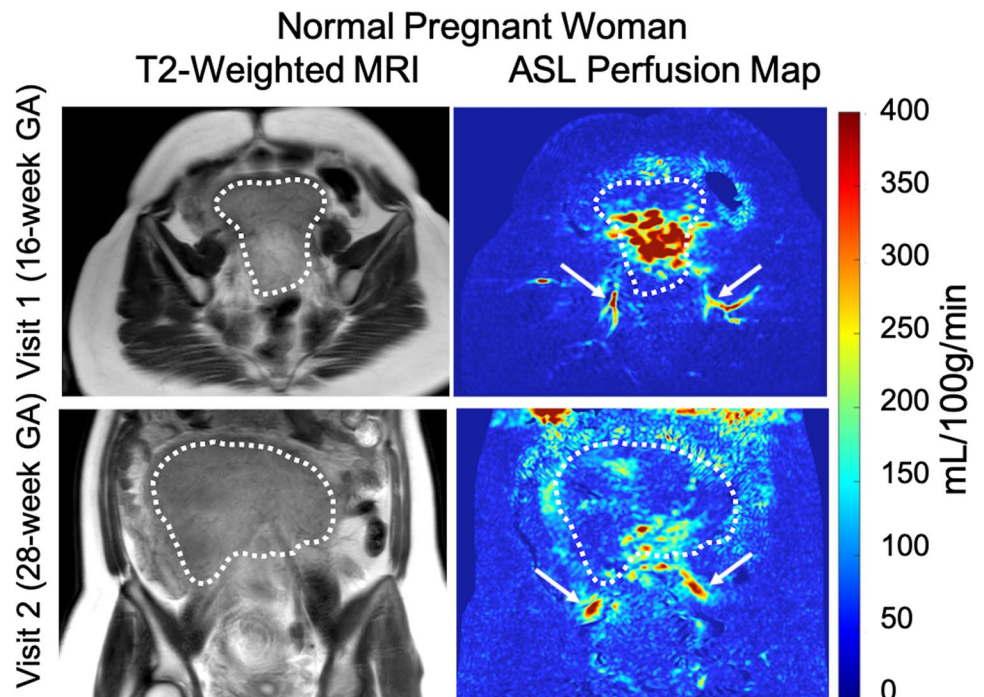
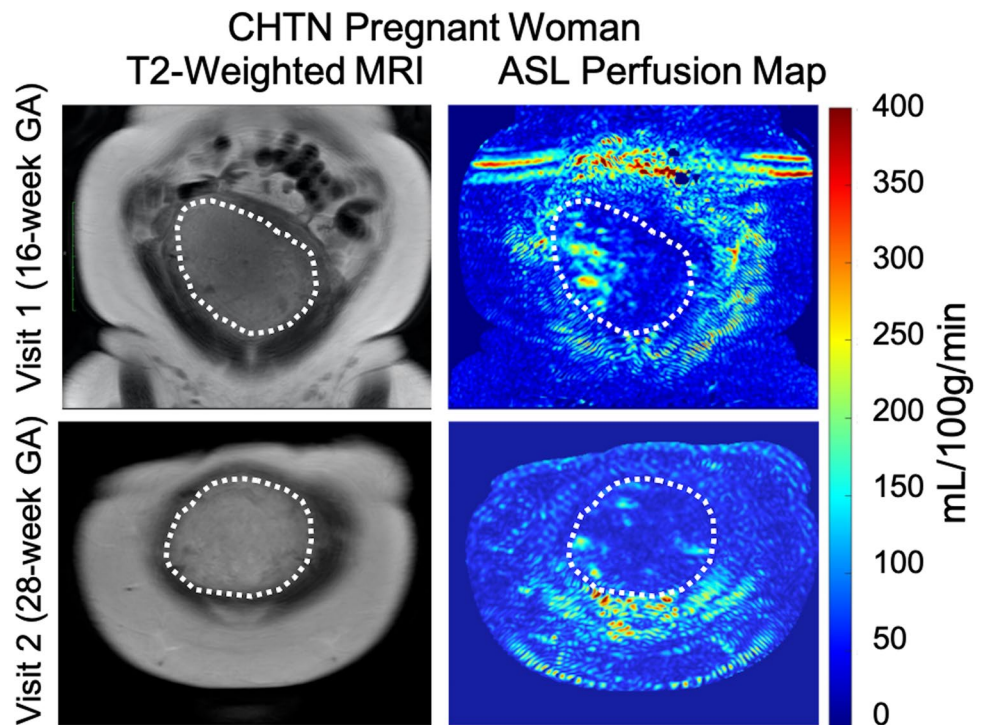


Fig. 4 T2-weighted images (left) and ASL perfusion map (right) acquired at the same imaging slice in a pregnant subject with chronic hypertension (cHTN), shown at 16-week (top row) and 28-week (bottom row) gestational ages (GA) respectively. The white dotted line outlines the placenta, drawn on the T2-weighted image and copied over to perfusion map. The placental blood flow at visit 1 (top row) was 68 ± 47 mL/100 g/min and at visit 2 (bottom row) was 53 ± 36 mL/100 g/min in this cHTN subject



complications had a similar trend to normal pregnant subjects, possibly providing an imaging biomarker for patient management.

Our baseline rates of PBF are in line with previously published results. The recent work by Liu et al. found PBF using pCASL-MRI in normal subjects at 16 weeks and 20 weeks of gestational age as 104.9 ± 31.4 and 111.3 ± 25.9 mL/100 g/min respectively [9]. Liu and colleagues also examined subjects with ischemic placenta disease represented by gestational hypertension, preeclampsia with or without severe features, and fetal growth restriction/small for gestational age. In this more heterogenous group, PBF was 97.2 ± 25.3 and 106.6 ± 22.3 mL/100 g/min at 16 and 20 weeks of gestational age respectively. Our values are perhaps lower than those reported by other ASL techniques, though variation may be accounted for by variation in ASL techniques, subject positioning (supine versus lateral), population characteristics, and gestational age of imaging (Table 3) [6, 9, 27]. In addition, the assumptions used in a particular ASL model may cause errors among different ASL techniques; however, such error is likely to be systematic and should not induce significant differences when assessing pathology using the same technique [9].

Similar to Zun et al., we observed a decrease in perfusion in normal placentas in the supine position over time [6]. Previously, this has been postulated due to an effect that may be mediated by the increased weight of the uterus on vena caval return; however, a recent study by Hughes et al. did not find a difference in IVC flow when the left lateral decubitus position was compared to the supine position [21].

In fact, the spinal venous plexus acts as a complementary venous return system maintaining vascular hemostasis. Further investigation is thus needed to determine the etiology of this perfusion decrease.

To our knowledge, there are no studies that specifically use ASL to address perfusion in the chronic hypertensive placenta (MEDLINE search for “ASL” or “arterial spin

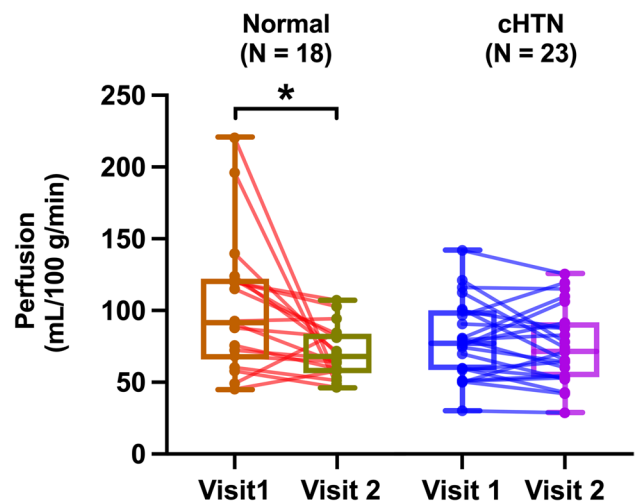


Fig. 5 Box-whisker plots of mean quantitative placental perfusion values of 18 normal pregnant subjects (left) and 23 pregnant subjects with chronic hypertension requiring antihypertensive therapy (cHTN, right). The values at visit 1 (16–20-week gestational age) and visit 2 (24–28-week gestational age) of the same subject are connected by solid lines. *Statistically significant decrease in perfusion between the two time points ($p=0.004$)

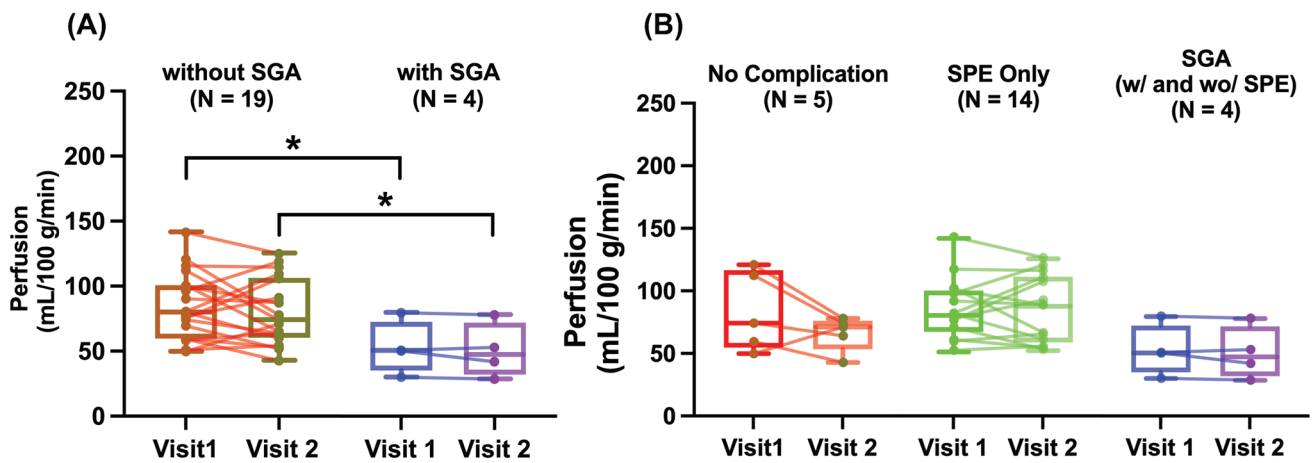


Fig. 6 Sub-cohort analysis of 23 pregnant subjects with chronic hypertension. **A** Box-whisker plots of mean quantitative placental perfusion stratified by subjects who had small for gestational age (SGA) infant ($N = 4$) compared to subjects without SGA ($N = 19$). *Statistically significant difference in perfusion at visit 1 ($p = 0.027$) and at visit 2 ($p = 0.044$). **B** Box-whisker plots of mean quantitative

placental perfusion stratified by no additional placental-mediated complications ($N = 5$), subjects who developed preeclampsia with severe features only (SPE, $N = 14$), and subjects who had SGA infant ($N = 2$ with SPE and 2 without SPE). The values at visit 1 (16–20-week gestational age) and visit 2 (24–28-week gestational age) of the same subject are connected by solid lines

labeling” and “pregnancy” and “chronic hypertension”). We observed that perfusion remained relatively constant over time in this cohort. It has been previously suggested through pathologic study that placentas with vascular disease have defective spiral artery remodeling [28]. We hypothesize that the lack of change in perfusion may be indicative of this defective remodeling in subjects with cHTN, the severity

of which can lead to fetal growth restriction/small for gestational age infant as observed with significantly lower perfusion in this cohort with the most extreme subtype. The remodeling observed has been suggested to typically preserve the placental bed near the cord insertion while compromising vessels at the periphery [28, 29]; therefore, future study will focus on regional variation and histogram analysis

Table 3 Placenta perfusion measurements reported in literature using ASL

Author	Technique	Gestational age (weeks)	Population	Subject position	Perfusion (mL/100 g/min)
Gowland 1998 [27]	0.5 T EPI	31 ± 6	Normal ($N = 15$)	Unknown	176 ± 24
Morris 2012 [31]	0.5 T FAIR ASL	3rd trimester	Normal ($N = 9$)	Unknown	111 ± 29
Zun 2017 [6]	1.5 T VS-ASL	32 ± 5	Normal ($N = 31$)	16 supine 15 lateral	171 ± 32 207 ± 39
Shao 2018 [8]	3 T 3D GRASE pCASL	14–16 19–22	Normal ($N = 34$)	Unknown	105.9 ± 26.5 116.9 ± 25.7
Link 2021 [32]	3 T 3D GRASE pCASL	32.4 ± 0.6 35.5 ± 1.8	Normal ($N = 12$) FGR ($N = 5$)	Unknown	147 ± 9.4 142.6 ± 23.5
Liu 2020 [9]	3 T pCASL	15.6 ± 1.0 20.8 ± 1.3	Normal ($N = 54$)	Supine	104.9 ± 31.4 111.3 ± 25.9
Our study	3 T pCASL	15.7 ± 1.0	IPD ($N = 15$)	Supine	97.2 ± 25.3
		20.2 ± 1.2			106.6 ± 22.3
		18.0 ± 1.1	Normal ($N = 18$)	Supine	103.1 ± 48.0
		26.4 ± 1.3			71.4 ± 18.3
		18.3 ± 1.4	cHTN ($N = 23$)	Supine	79.4 ± 27.4
		26.5 ± 1.1			74.9 ± 26.6

ASL, arterial spin labeling; EPI, echo planar imaging; FAIR, flow-sensitive alternating inversion recovery; VS, velocity-selective; IPD, ischemic placental disease (3 gestational hypertension, 5 preeclampsia, 3 fetal growth restriction/small for gestational age, 2 preterm birth, 2 combination of these diagnoses); pCASL, pseudo-continuous ASL

in placental perfusion given that changes in global perfusion were not observed.

This idea of regionalization is also supported by the observed spatial variation of perfusion signal with focal hyperintensities on placental perfusion maps, which have also been previously observed [9]. Spatial variation may well represent the vascular structure of the placenta, specifically the placental cotyledons, that may also enable future assessment of placental insufficiency in pathology in a region-specific manner. This would explain that while global perfusion is preserved, regional perfusion may be more indicative of disease pathology and will be an area of interest in future study.

We did not observe any perfusion difference with those subjects with chronic hypertension who went on to develop SPE. However, in this cohort there were only 5 cases of early-onset SPE (at 30w0d, 31w2d, 31w3d, 32w6d, and 33w5d respectively), so it is possible that differences in perfusion were not captured based on our early time points of interest.

This study has some limitations. First, given that hypertension incidence increases with age and obesity, the pregnant subjects with cHTN were older, more parous, and more obese than the normal pregnant subjects in our cohort, which may contribute to bias. However, the perfusion difference between normal pregnant subjects and pregnant subjects with cHTN seems to arise primarily due to hypertension and not from differences in body mass index (BMI). This is because the difference in placental perfusion between these two groups was not statistically significant while the BMI differences were statistically significant at both visits (Table 2). Future studies will also consider the effects of BMI on placental perfusion measurements. Second, our sample size was small in the current study with 52 pregnant subjects. This represents the preliminary evaluation in our ongoing large-scale study, where we plan to enroll 100 normal and 100 cHTN pregnancies for a total sample size of 200 subjects. This sample size was calculated to provide a minimal detectable effect size of 0.5 with 80% power at a significance level of 0.01 (performed with Bonferroni correction due to multiple measurements). This larger sample size is warranted to confirm the significant differences that we observed by clinical outcome. Third, our pCASL-MRI were performed during free breathing; however, the use of SSHTSE acquisition combined with background suppression minimized the breathing artifacts. Future studies will also incorporate motion registration algorithms to further minimize breathing artifacts. Next, we used only 4 NSAs for each slice and 5 slices to cover the entire placenta. Higher NSAs could potentially increase the signal to noise ratio, however at the expense of longer scan times. Finally, the manual segmentation on the T2-weighted images with matching slice thickness and orientation to the ASL images also contributes to partial volume effects in the PBF maps. Future work using automated segmentation methods [30] will try to minimize partial volume effects and can also provide objective measurements.

In conclusion, we demonstrated that placental perfusion measurements in normal pregnancy and in those affected by chronic hypertension can be assessed longitudinally using pCASL-MRI. We observed mean placental perfusion was not statistically different in subjects with chronic hypertension compared to normal subjects at 16–20 or 24–28 weeks of gestational age, in this limited cohort. Placental perfusion in the second trimester declined in normal pregnant subjects whereas it remained relatively unchanged in pregnant subjects with chronic hypertension, suggesting a compensatory mechanism that preserves function. Perfusion was significantly lower in those with small for gestational age infants, indicating that pCASL-MRI-measured perfusion may be an effective imaging biomarker for placental insufficiency.

Acknowledgements The authors thank all subjects for their participation in the study; and Sydney Haldeman, MPH; Vida Rhodes, BBA, LVN; and Abey Thomas, RTR, MR, for their help and support in the recruitment and scanning of all subjects.

The subjects reported in this study represent the preliminary evaluation in our ongoing large-scale study, where we plan to enroll 100 normal and 100 cHTN pregnancies for a total sample size of 200 subjects. This sample size was calculated to provide a minimal detectable effect size of 0.5 with 80% power at a significance level of 0.01 (performed with Bonferroni correction due to multiple measurements).

Funding The authors state that this work has not received any funding.

CLH is supported by the Eunice Kennedy Shriver National Institute of Child Health and Human Development (NICHD) of the National Institutes of Health (NIH) under award number K23HD103876.

Declarations

Guarantor The scientific guarantor of this publication is Ananth Mahuranthakam, PhD.

Conflict of interest The authors of this manuscript declare no relationships with any companies, whose products or services may be related to the subject matter of the article.

Statistics and biometry One of the authors (Yin Xi) has significant statistical expertise.

Informed consent Written informed consent was obtained from all subjects (patients) in this study.

Ethical approval Institutional Review Board approval was obtained.

Study subjects or cohorts overlap None of the study subjects or cohorts has been previously reported in publications. However, the subjects reported in this study represent the preliminary evaluation in our ongoing large-scale study, where we plan to enroll 100 normal and 100 cHTN pregnancies for a total sample size of 200 subjects. This sample size was calculated to provide a minimal detectable effect size of 0.5 with 80% power at a significance level of 0.01 (performed with Bonferroni correction due to multiple measurements).

Methodology

- prospective
- case–control study/observational study
- performed at one institution

References

- Harris LK, Benagiano M, D'Elios MM, Brosens I, Benagiano G (2019) Placental bed research: II. Functional and immunological investigations of the placental bed. *Am J Obstet Gynecol* 221:457–469
- Fisher S, McMaster M, Roberts JM (2015) The placenta in normal pregnancy and preeclampsia. In: Taylor RNRJ, Cunningham FG, Lindheimer MD (eds) *Chesley's hypertensive disorders in pregnancy*. Elsevier, San Diego
- Combs CA, Katz MA, Kitzmiller JL, Brescia RJ (1993) Experimental preeclampsia produced by chronic constriction of the lower aorta: validation with longitudinal blood pressure measurements in conscious rhesus monkeys. *Am J Obstet Gynecol* 169:215–223
- Papageorghiou AT, Yu CK, Nicolaides KH (2004) The role of uterine artery Doppler in predicting adverse pregnancy outcome. *Best Pract Res Clin Obstet Gynaecol* 18:383–396
- Myatt L, Clifton RG, Roberts JM et al (2012) The utility of uterine artery Doppler velocimetry in prediction of preeclampsia in a low-risk population. *Obstet Gynecol* 120:815–822
- Zun Z, Zaharchuk G, Andescavage NN, Donofrio MT, Limperopoulos C (2017) Non-invasive placental perfusion imaging in pregnancies complicated by fetal heart disease using velocity-selective arterial spin labeled MRI. *Sci Rep* 7:16126
- Zun Z, Limperopoulos C (2018) Placental perfusion imaging using velocity-selective arterial spin labeling. *Magn Reson Med* 80:1036–1047
- Shao X, Liu D, Martin T et al (2018) Measuring human placental blood flow with multidelay 3D GRASE pseudocontinuous arterial spin labeling at 3T. *J Magn Reson Imaging* 47:1667–1676
- Liu D, Shao X, Danyalov A et al (2020) Human placenta blood flow during early gestation with pseudocontinuous arterial spin labeling MRI. *J Magn Reson Imaging* 51:1247–1257
- Harteveld AA, Hutter J, Franklin SL et al (2020) Systematic evaluation of velocity-selective arterial spin labeling settings for placental perfusion measurement. *Magn Reson Med* 84:1828–1843
- Seely EW, Ecker J (2014) Chronic hypertension in pregnancy. *Circulation* 129:1254–1261
- Zeeman GG, McIntire DD, Twickler DM (2003) Maternal and fetal artery Doppler findings in women with chronic hypertension who subsequently develop superimposed pre-eclampsia. *J Matern Fetal Neonatal Med* 14:318–323
- Browne JC, Veall N (1953) The maternal placental blood flow in normotensive and hypertensive women. *J Obstet Gynaecol Br Emp* 60:141–147
- Brosens JJ, Pijnenborg R, Brosens IA (2002) The myometrial junctional zone spiral arteries in normal and abnormal pregnancies: a review of the literature. *Am J Obstet Gynecol* 187:1416–1423
- ACOG (2017) Committee opinion no 700: methods for estimating the due date. *Obstet Gynecol* 129:e150–e154
- ACOG (2020) Practice bulletin no 222: gestational hypertension and preeclampsia. *Obstet Gynecol* 135:1492–1495
- ACOG (2021) Practice bulletin no 227: fetal growth restriction. *Obstet Gynecol* 137:385–387
- Duryea EL, Hawkins JS, McIntire DD, Casey BM, Leveno KJ (2014) A revised birth weight reference for the United States. *Obstet Gynecol* 124:16–22
- Chappell LC, Enye S, Seed P, Briley AL, Poston L, Shennan AH (2008) Adverse perinatal outcomes and risk factors for preeclampsia in women with chronic hypertension: a prospective study. *Hypertension* 51:1002–1009
- Sibai BM (2002) Chronic hypertension in pregnancy. *Obstet Gynecol* 100:369–377
- Hughes EJ, Price AN, McCabe L et al (2021) The effect of maternal position on venous return for pregnant women during MRI. *NMR Biomed* 34:e4475
- Alsop DC, Detre JA, Golay X et al (2015) Recommended implementation of arterial spin-labeled perfusion MRI for clinical applications: a consensus of the ISMRM perfusion study group and the European consortium for ASL in dementia. *Magn Reson Med* 73:102–116
- Greer JS, Wang X, Wang Y et al (2019) Robust pCASL perfusion imaging using a 3D Cartesian acquisition with spiral profile reordering (CASPR). *Magn Reson Med* 82:1713–1724
- Robson PM, Madhuranthakam AJ, Dai W, Pedrosa I, Rofsky NM, Alsop DC (2009) Strategies for reducing respiratory motion artifacts in renal perfusion imaging with arterial spin labeling. *Magn Reson Med* 61:1374–1387
- Zhang Y, Kapur P, Yuan Q et al (2016) Tumor vascularity in renal masses: correlation of arterial spin-labeled and dynamic contrast-enhanced magnetic resonance imaging assessments. *Clin Genitourin Cancer* 14:e25–36
- Wang X, Greer JS, Dimitrov IE, Pezeshk P, Chhabra A, Madhuranthakam AJ (2018) Frequency offset corrected inversion pulse for B0 and B1 insensitive fat suppression at 3T: application to MR neurography of brachial plexus. *J Magn Reson Imaging* 48:1104–1111
- Gowland PA, Francis ST, Duncan KR et al (1998) In vivo perfusion measurements in the human placenta using echo planar imaging at 0.5 T. *Magn Reson Med* 40:467–473
- Brosens I, Pijnenborg R, Vercruyse L, Romero R (2011) The “great obstetrical syndromes” are associated with disorders of deep placentation. *Am J Obstet Gynecol* 204:193–201
- Brosens I, Puttemans P, Benagiano G (2019) Placental bed research: I. The placental bed: from spiral arteries remodeling to the great obstetrical syndromes. *Am J Obstet Gynecol* 221:437–456
- Shahedi M, Spong CY, Dormer JD et al (2021) Deep learning-based segmentation of the placenta and uterus on MR images. *J Med Imaging (Bellingham)* 8:054001
- Morris D, Wright C, Dobbs M et al (2012) Arterial spin labeling in the human placenta—mapping perfusion Proc 20th Annual Meeting ISMRM, Melbourne
- Link D, Avisdris N, Shao X et al (2021) Multi-parametric functional and structural assessment of the placenta at late gestational ages using MRI. Proc 2021 Annual Meeting ISMRM, Virtual, p 3883

Publisher's note Springer Nature remains neutral with regard to jurisdictional claims in published maps and institutional affiliations.

Springer Nature or its licensor (e.g. a society or other partner) holds exclusive rights to this article under a publishing agreement with the author(s) or other rightsholder(s); author self-archiving of the accepted manuscript version of this article is solely governed by the terms of such publishing agreement and applicable law.